# Time evolution, Lamb shift, and emission spectra of spontaneous emission of two identical atoms

Da-wei Wang,[1] Zheng-hong Li,[2] Hang Zheng,[3] and Shi-yao Zhu[1,2]

[1]*Center of Optical Sciences and Department of Physics, The Chinese University of Hong Kong, N.T., Hong Kong, People's Republic of China*

[2]*Department of Physics, Hong Kong Baptist University, Kowloon Tong, Hong Kong, People's Republic of China*

[3]*Department of Physics, Shanghai Jiao Tong University, Shanghai 200030, People's Republic of China*

(Received 14 January 2010; published 15 April 2010)

A unitary transformation method is used to investigate the dynamic evolution of two multilevel atoms, in the basis of symmetric and antisymmetric states, with one atom being initially prepared in the first excited state and the other in the ground state. The unitary transformation guarantees that our calculations are based on the ground state of the atom-field system and the self-energy is subtracted at the beginning. The total Lamb shifts of the symmetric and antisymmetric states are divided into transformed shift and dynamic shift. The transformed shift is due to emitting and reabsorbing of virtual photons, by a single atom (nondynamic single atomic shift) and between the two atoms (quasi-static shift). The dynamic shift is due to the emitting and reabsorbing of real photons, by a single atom (dynamic single atomic shift) and between the two atoms (dynamic interatomic shift). The emitting and reabsorbing of virtual and real photons between the two atoms result in the interatomic shift, which does not exist for the one-atom case. The spectra at the long-time limit are calculated. If the distance between the two atoms is shorter than or comparable to the wavelength, the strong coupling between the two atoms splits the spectrum into two peaks, one from the symmetric state and the other from the antisymmetric state. The origin of the red or blue shifts for the symmetric and antisymmetric states mainly lies in the negative or positive interaction energy between the two atoms. In the investigation of the short time evolution, we find the modification of the effective density of states by the interaction between two atoms can modulate the quantum Zeno and quantum anti-Zeno effects in the decays of the symmetric and antisymmetric states.

DOI: 10.1103/PhysRevA.81.043819 PACS number(s): 42.50.Ct, 42.50.Nn, 03.65.Xp

## I. INTRODUCTION

The coherence between many identical two-level atoms was first investigated by Dicke in 1954 [1], where the concepts of superradiant and subradiant states were introduced to describe two kinds of coherence between atoms. The superradiant state has an enhanced decay rate and a shorter lifetime compared with a single excited atom, while the subradiant state has an inhibited decay rate and a longer lifetime. The subradiant state is thus a very good candidate for preserving quantum information, and, therefore, the coherence between atoms has retriggered much interest recently, especially the shift and spectra of the coherent system [2–4].

The distance between the atoms cannot be neglected in the study of the energy shift induced by the interaction between atoms, but it is somewhat difficult to take the distance into account. The simplest model is the system composed of two two-level atoms, which was first analytically calculated [5] with the initial condition in which one atom is in the excited state and the other in the ground state, where the rotating wave approximation (RWA) is used due to the basis the authors have chosen. The authors [5] obtained two peaks in the spectra: one wide peak from the symmetric state and one narrow peak from the antisymmetric state. In Ref. [6], the counter-rotating terms were taken into account by exact integration of the Heisenberg equation. Later, by using the density matrix and the projection operator technique, the same answer is recalculated with the master equation method [7]. Most of the studies thereafter [3,8] are based on these two approaches in Refs. [6,7].

The Weisskopf-Wigner approach is usually used to investigate the dynamic evolution of probability amplitude. However, in this approach, one needs to start with the ground state of the whole Hamiltonian including the counter-rotating terms, which makes the calculation very complicated [4]. One of the objects of this paper is to make the Weisskopf-Wigner approach work with a simple calculation in the system of two multilevel atoms by a unitary transformation method [9].

In quantum optics, unitary transformation is a usual method to simplify the Hamiltonian [10]. Previously, we have investigated the dynamic evolution of a hydrogen atom with the unitary transformation method, which can effectively take into account the counter-rotating terms [9]. The Lamb shift of a single atom is also calculated with this method [11], where the same result as the one of Bethe [12] is obtained. In this paper, we extend this method to two multilevel atoms, and we will show that the same result as in Refs. [6] and [7] can be obtained with the Weisskopf-Wigner approach. Therefore, another main point of this paper is to incorporate the Lamb shift naturally into the calculation and to investigate the short-time evolution of the symmetric and antisymmetric states. Compared with the single-atom case, the symmetric and antisymmetric states of two atoms feel some modulation of the electromagnetic density of states (DOS). Besides the well-known modification of long-time decay rate [1], this will also greatly modify the short-time evolution.

This paper is prepared as follows: In Sec. II, we give the unitary transformation of the Hamiltonian of the system composed of two multilevel atoms and radiation fields. We also introduce symmetric and antisymmetric states as the basis and their shifts after the transformation are calculated. In Sec. III, we derive the general formulas of the dynamic evolution. In Sec. IV, the long-time evolution is discussed in detail, including the decay rates, shifts, and spectra. The classical correspondence of the blue and red shifts in the

 

spectra is discussed to help understand the physics. In Sec. V, we calculate the short-time evolution of the system, and Sec. VI is a summary.

## II. TRANSFORMATION OF THE HAMILTONIAN AND THE BASIS

We investigate the dynamic evolution of two multilevel atoms. By adopting the minimal coupling interaction, the total Hamiltonian of the atoms and electromagnetic (EM) fields can be written as ($\hbar = 1$) [7]

$$H = H_0 + H_I + H_{d-d}, \tag{1}$$

where

$$H_0 = \sum_{j=1,2}\sum_{l} \omega_l |l\rangle_j\langle l|_j + \sum_{\mathbf{k}} \omega_k b_{\mathbf{k}}^\dagger b_{\mathbf{k}}, \tag{2}$$

$$H_I = \sum_{j=1,2}\sum_{l,m;\mathbf{k}} g_{\mathbf{k};lm}|l\rangle_j\langle m|_j(b_{\mathbf{k}}^\dagger e^{-i\mathbf{k}\cdot\mathbf{r}_j} + b_{\mathbf{k}} e^{i\mathbf{k}\cdot\mathbf{r}_j}), \tag{3}$$

$$H_{d-d} = \frac{1}{4\pi\varepsilon_0}\left[\frac{\mathbf{d}^{(1)}\cdot\mathbf{d}^{(2)}}{r_{12}^3} - \frac{3(\mathbf{d}^{(1)}\cdot\mathbf{r}_{12})(\mathbf{d}^{(2)}\cdot\mathbf{r}_{12})}{r_{12}^5}\right]. \tag{4}$$

$H_0$ is the unperturbed Hamiltonian of the atoms and fields, $H_I$ is the interaction Hamiltonian between the atoms and transverse fields, and $H_{d-d}$ is the electrostatic interaction between the atoms. Here $\omega_l$ is the eigenenergy of the $l$th eigenstate $|l\rangle_j$ of the $j$th atom, $\omega_k$ is the frequency of the $\mathbf{k}$th EM mode (with the summation over $\mathbf{k}$ including the two polarizations), and $g_{\mathbf{k};lm} = \omega_{lm} d_{lm}(2\varepsilon_0\omega_k V_q)^{-1/2}\hat{\mathbf{e}}_{\mathbf{k}}\cdot\hat{\mathbf{u}}_{lm}$ (with $V_q$ the quantization volume) is the coupling constant between the $\mathbf{k}$th EM mode with unit polarization vector $\hat{\mathbf{e}}_{\mathbf{k}}$ and the atomic transition between levels $|l\rangle$ and $|m\rangle$ with transition dipole moment $\mathbf{d}_{lm} = e\langle l|\mathbf{r}|m\rangle = d_{lm}\hat{\mathbf{u}}_{lm}$, of which $d_{lm}$ (assumed to be real) and $\hat{\mathbf{u}}_{lm}$ are the magnitude and unit vector, respectively. $b_{\mathbf{k}}$ and $b_{\mathbf{k}}^\dagger$ are the annihilation and creation operators of the $\mathbf{k}$th mode. The two atoms are located at $\mathbf{r}_1$ and $\mathbf{r}_2$ and their displacement is $\mathbf{r}_{12} = \mathbf{r}_1 - \mathbf{r}_2$. In Eq. (4), $\mathbf{d}^{(j)} = \sum_{lm}\mathbf{d}_{lm}|l\rangle_{jj}\langle m|$ is the dipole moment of the $j$th atom. The angle between the dipole (assuming the same direction for the two atoms) and $\mathbf{r}_{21}$ is $\eta$, as shown in Fig. 1.

In order to take into account the counter-rotating terms and the self-energy at the beginning because it is always there, we extend the unitary transformation method developed in Ref. [9] to the two-atom case under investigation. Making the unitary transformation and subtracting the self-energy, $H^S = e^{iS}He^{-iS} - E_{\rm se}$ ($E_{\rm se} = -\sum_{j,m\neq l}\sum_{\mathbf{k}}|g_{\mathbf{k};lm}|^2/\omega_k|l\rangle_j\langle l|_j$), where

$$S = \sum_{j=1,2}\sum_{l,m;\mathbf{k}}\frac{g_{\mathbf{k};lm}\xi_{k;lm}}{i\omega_k}|l\rangle_j\langle m|_j(b_{\mathbf{k}}^\dagger e^{-i\mathbf{k}\cdot\mathbf{r}_j} - b_{\mathbf{k}}e^{i\mathbf{k}\cdot\mathbf{r}_j}), \tag{5}$$

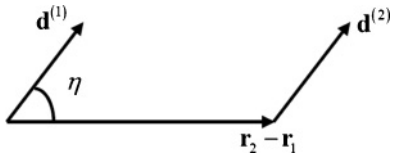


FIG. 1. The schematic description of the relation between dipoles and displacements.

with $\xi_{k;lm} = \frac{\omega_k}{\omega_k + |\omega_{lm}|}$ and $\omega_{lm} = \omega_l - \omega_m$, we obtain

$$H^S = H_0 + (H_0' - E_{\rm se}) + H_I' + H_{ia} + H_{d-d}, \tag{6}$$

where

$$H_0 = \sum_{j=1,2}\sum_{l}\omega_l|l\rangle_j\langle l|_j + \sum_{\mathbf{k}}\omega_{\mathbf{k}}b_{\mathbf{k}}^\dagger b_{\mathbf{k}}, \tag{7}$$

$$H_0' - E_{\rm se} = \sum_{j=1,2,\mathbf{k}}\sum_{l,m}\frac{|g_{\mathbf{k};lm}|^2}{\omega_k} \times\left(\xi_{k;lm}^2 - 2\xi_{k;lm} - \frac{\omega_{lm}}{\omega_k}\xi_{k;lm}^2 + 1\right)|l\rangle_j\langle l|_j, \tag{8}$$

$$H_I' = \sum_{j=1,2,\mathbf{k}}\sum_{l>m}V_{lm,\mathbf{k}}(|l\rangle_j\langle m|_j b_{\mathbf{k}}e^{i\mathbf{k}\cdot\mathbf{r}_j} + |m\rangle_j\langle l|_j b_{\mathbf{k}}^\dagger e^{-i\mathbf{k}\cdot\mathbf{r}_j}), \tag{9}$$

$$H_{ia} = -\sum_{l,l',m,m';\mathbf{k}}\frac{2g_{\mathbf{k};lm}g_{\mathbf{k};l'm'}\xi_{k;lm}}{\omega_k}(2-\xi_{k;l'm'})|l\rangle_1\langle m|_1 \otimes|l'\rangle_2\langle m'|_2 e^{i\mathbf{k}\cdot\mathbf{r}_{12}}. \tag{10}$$

$H_0' - E_{\rm se}$ only contains diagonal energy corrections (nondynamic shift) [11] for a single atom. In the transformed basis, $H_I'$ is the interaction Hamiltonian for a single atom due to real photon emission and $V_{lm,\mathbf{k}} = g_{lm,\mathbf{k}}\frac{2|\omega_{lm}|}{\omega_k+|\omega_{lm}|}$ is the transformed coupling strength. $H_{ia}$ is the interaction Hamiltonian between two atoms due to exchange of virtual photons (here called the quasi-static interaction). Note that in the transformed basis, $H_I'$ has a RWA-like form, and $H_{d-d}$ does not change its form after the transformation because it commutes with $S$.

We suppose the distance between two atoms is large enough so that their wave functions have no overlap, and thus we need not worry about the identical property of the two atoms. The foregoing derivation of the effective Hamiltonian in Eqs. (6)–(10) is valid for all transitions between any levels. We take the simplest example that the system is initially prepared in the state which on average has one atom in the first excited state and the other in the ground state. In this case, the results can be easily tested because this has been well studied [6]. We expand the wave function on the basis of symmetric and antisymmetric states:

$$|s\rangle = \frac{\sqrt{2}}{2}(|e,g\rangle + |g,e\rangle), \tag{11}$$

$$|a\rangle = \frac{\sqrt{2}}{2}(|e,g\rangle - |g,e\rangle), \tag{12}$$

where $|e,g\rangle$ means that the first atom is in the first excited state and the second atom is in the ground state of the atom-field system [11]. The system is initially prepared as a superposition of a symmetric and an antisymmetric state with no photons in vacuum [i.e., $|\Psi(0)\rangle = C_a(0)|a;\{0_{\mathbf{k}}\}\rangle + C_s(0)|s;\{0_{\mathbf{k}}\}\rangle$, where we denote the vacuum state as $|\{0_{\mathbf{k}}\}\rangle$]. After some time, it may decay to the ground state and emit one photon into the $\mathbf{k}$th mode; that is, the system transits to the state $|g,g;1_{\mathbf{k}}\rangle$. Note that in the untransformed basis, states like $|e,e;1_{\mathbf{k}}\rangle$ may be generated by the counter-rotating terms and the calculations are complicated [4]. As $H_0 + H_0' - E_{\rm se}$ does not depend on the position, its contribution to the energies of $|s\rangle$ and $|a\rangle$ is

also independent of the position; these energies are

$$\langle s|H_0+H_0'-E_{\rm se}|s\rangle = \langle a|H_0+H_0'-E_{\rm se}|a\rangle = \omega_g+\omega_e+E_g^{\rm nd}+E_e^{\rm nd}, \quad (13)$$

$$\langle g,g|H_0+H_0'-E_{\rm se}|g,g\rangle = 2\omega_g+2E_g^{\rm nd}, \quad (14)$$

where

$$E_l^{\rm nd}=\sum_{m\neq l,\mathbf{k}}\frac{|g_{\mathbf{k};lm}|^2}{\omega_k}\left(\xi_{k;lm}^2-2\xi_{k;lm}-\frac{\omega_{lm}}{\omega_k}\xi_{k;lm}^2+1\right), \quad (l,m=e,g). \quad (15)$$

Note that $E_l^{\rm nd}$ is the nondynamic shift for the single-atom state $|l\rangle$ [11]. The nondynamic shifts for the states $|a\rangle$ and $|s\rangle$ are the same (one from the excited state and the other from the ground state), equal to $E_s^{\rm nd}=E_a^{\rm nd}=E_e^{\rm nd}+E_g^{\rm nd}$. In the symmetric and antisymmetric basis, the electrostatic Hamiltonian $H_{d-d}$ is diagonal:

$$\langle s|H_{d-d}|s\rangle = -\langle a|H_{d-d}|a\rangle = E_{d-d} = \frac{1}{4\pi\varepsilon_0}\left[\frac{\mathbf{d}_{eg}^{(1)}\cdot\mathbf{d}_{ge}^{(2)}}{r_{12}^3}-\frac{3\left(\mathbf{d}_{eg}^{(1)}\cdot\mathbf{r}_{12}\right)\left(\mathbf{d}_{ge}^{(2)}\cdot\mathbf{r}_{12}\right)}{r_{12}^5}\right], \quad (16)$$

$$\langle s|H_{d-d}|a\rangle = \langle s|H_{d-d}|a\rangle = 0. \quad (17)$$

In addition, the transformed interatomic Hamiltonian $H_{ia}$ is also diagonal:

$$\langle s|H_{ia}|s\rangle = -\langle a|H_{ia}|a\rangle = E_{ia} = -\sum_{\mathbf{k}}\frac{2|g_{\mathbf{k};eg}|^2\xi_{k;eg}}{\omega_k}(2-\xi_{k;eg})e^{i\mathbf{k}\cdot\mathbf{r}_{12}}, \quad (18)$$

$$\langle s|H_{ia}|a\rangle = \langle s|H_{ia}|a\rangle = 0. \quad (19)$$

Equations (16) and (18) tell us that due to the electrostatic dipole-dipole interaction $H_{d-d}$ and the quasi-static interaction $H_{ia}$, the energies of $|a\rangle$ and $|s\rangle$ split with opposite shifts,

$$\Delta E_s^{\rm sta}=-\Delta E_a^{\rm sta}=E_{d-d}+E_{ia}, \quad (20)$$

which are dependent on $\mathbf{r}_1$ and $\mathbf{r}_2$. The interaction Hamiltonian $H_I'$ has the matrix elements

$$\langle g,g;1_{\mathbf{k}}|H_I'|s;\{0_{\mathbf{k}}\}\rangle = \frac{1}{\sqrt{2}}V_{eg,\mathbf{k}}(e^{-i\mathbf{k}\cdot\mathbf{r}_1}+e^{-i\mathbf{k}\cdot\mathbf{r}_2}), \quad (21)$$

$$\langle g,g;1_{\mathbf{k}}|H_I'|a;\{0_{\mathbf{k}}\}\rangle = \frac{1}{\sqrt{2}}V_{eg,\mathbf{k}}(e^{-i\mathbf{k}\cdot\mathbf{r}_1}-e^{-i\mathbf{k}\cdot\mathbf{r}_2}). \quad (22)$$

We would like to emphasize that the second-order effective interaction Hamiltonian between $|s;\{0_{\mathbf{k}}\}\rangle$ and $|a;\{0_{\mathbf{k}}\}\rangle$ is zero because

$$\sum_{\mathbf{k}}\langle a;\{0_{\mathbf{k}}\}|H_I'|g,g;1_{\mathbf{k}}\rangle\langle g,g;1_{\mathbf{k}}|H_I'|s;\{0_{\mathbf{k}}\}\rangle = \frac{1}{2}\sum_{\mathbf{k}}|V_{eg,\mathbf{k}}|^2[e^{i\mathbf{k}\cdot(\mathbf{r}_1-\mathbf{r}_2)}-e^{-i\mathbf{k}\cdot(\mathbf{r}_1-\mathbf{r}_2)}]=0, \quad (23)$$

where the summation of the second term in the square brackets, $e^{-i\mathbf{k}\cdot(\mathbf{r}_1-\mathbf{r}_2)}$, is the same as the first one if we change the dummy index from $\mathbf{k}$ to $-\mathbf{k}$. Therefore, there are no interference effects between the states $|s;\{0_{\mathbf{k}}\}\rangle$ and $|a;\{0_{\mathbf{k}}\}\rangle$.

## III. DYNAMIC EVOLUTION

We take all the Hamiltonians except $H_I'$ as the unperturbed Hamiltonian, because they only have diagonal terms to the order of $d^2$. In the interaction picture, we suppose the wave function at time $t$ as

$$|\Psi(t)\rangle = C_a(t)|a;0_{\mathbf{k}}\rangle+C_s(t)|s;0_{\mathbf{k}}\rangle+\sum_{\mathbf{k}}C_{\mathbf{k}}(t)|g,g;1_{\mathbf{k}}\rangle. \quad (24)$$

The Schrödinger equation $i\dot{\Psi}(t)=\tilde{H}'\Psi(t)$ with $\tilde{H}'=e^{i(H_0+H_0'-E_{\rm se}+H_{ia}+V)t}H_I'e^{-i(H_0+H_0'-E_{\rm se}+H_{ia}+V)t}$ yields

$$i\dot{C}_a(t)=\sum_{\mathbf{k}}e^{i(\omega_{eg}'+\Delta E_a^{\rm sta}-\omega_k)t}\langle a;\{0_{\mathbf{k}}\}|H_I'|g,g;1_{\mathbf{k}}\rangle C_{\mathbf{k}}(t), \quad (25)$$

$$i\dot{C}_s(t)=\sum_{\mathbf{k}}e^{i(\omega_{eg}'+\Delta E_s^{\rm sta}-\omega_k)t}\langle s;\{0_{\mathbf{k}}\}|H_I'|g,g;1_{\mathbf{k}}\rangle C_{\mathbf{k}}(t), \quad (26)$$

$$i\dot{C}_{\mathbf{k}}(t)=e^{-i(\omega_{eg}'+\Delta E_a^{\rm sta}-\omega_k)t}\langle g,g;1_{\mathbf{k}}|H_I'|a;\{0_{\mathbf{k}}\}\rangle C_a(t)+e^{-i(\omega_{eg}'+\Delta E_s^{\rm sta}-\omega_k)t}\langle g,g;1_{\mathbf{k}}|H_I'|s;\{0_{\mathbf{k}}\}\rangle C_s(t), \quad (27)$$

where $\omega_{eg}'=\omega_e+E_e^{\rm nd}-\omega_g-E_g^{\rm nd}$ is the transformed transition frequency including the nondynamic shift. Integrating Eq. (27) and then substituting it in Eq. (25), we get

$$\dot{C}_a(t)=-\int_0^t dt'\sum_{\mathbf{k}}|\langle g,g;1_{\mathbf{k}}|H_I'|a;\{0_{\mathbf{k}}\}\rangle|^2\times e^{i(\omega_{eg}'+\Delta E_a^{\rm sta}-\omega_k)(t-t')}C_a(t') - \int_0^t dt'\sum_{\mathbf{k}}\langle a;\{0_{\mathbf{k}}\}|H_I'|g,g;1_{\mathbf{k}}\rangle\langle g,g;1_{\mathbf{k}}|H_I'|s;\{0_{\mathbf{k}}\}\rangle\times e^{i(\omega_{eg}'+\Delta E_a^{\rm sta}-\omega_k)t}e^{-i(\omega_{eg}'+\Delta E_s^{\rm sta}-\omega_k)t'}C_s(t'). \quad (28)$$

The second term in Eq. (28) is zero because of Eq. (23). [Note that the factor of $e^{-i\omega_k t}$ is the same for $\mathbf{k}$ and $-\mathbf{k}$, and has no effect on the result of the summation zero in Eq. (23).] An integral differential equation for $C_s(t)$ can be obtained in a similar way.

## IV. DECAY RATES, LAMB SHIFT, AND EMISSION SPECTRUM IN THE LONG-TIME LIMIT

We first investigate the case in the long-time limit, $t\gg 1/\Gamma_{a(s)}$, where $1/\Gamma_{a(s)}$ is the lifetime of the antisymmetric (symmetric) state. Because of the wide broadness of the vacuum spectrum, the correlation time is very short. We can approximate that the system has no memory, and replace $C_a(t')$ with $C_a(t)$ in Eq. (28) (the Markov approximation). Under the Weisskopf-Wigner approximation, extending the lower bound of time integration to $-\infty$ would not introduce much error:

$$\dot{C}_a(t)\approx -C_a(t)\int_{-\infty}^t dt'\sum_{\mathbf{k}}|\langle g,g;1_{\mathbf{k}}|H_I'|a;\{0_{\mathbf{k}}\}\rangle|^2\times e^{i(\omega_{eg}'+\Delta E_a^{\rm sta}-\omega_k)(t-t')}=-C_a(t)\left(\frac{\Gamma_a}{2}+i\delta_a\right), \quad (29)$$

in which the decay rate for the antisymmetric state is

$$\Gamma_a = 2\pi \sum_{\mathbf{k}} |\langle g,g;1_{\mathbf{k}}|H_I'|a;\{0_{\mathbf{k}}\}\rangle|^2 \delta\left(\omega_{eg}' + \Delta E_a^{\mathrm{sta}} - \omega_k\right)$$
$$= \Gamma_{eg}[1 - D(x_{12},\eta)], \tag{30}$$

with

$$D(x,\eta) = \frac{3}{2}\left\{\frac{\sin x}{x}\sin^2\eta + \frac{1-3\cos^2\eta}{x^2}\left[\cos x - \frac{\sin x}{x}\right]\right\}, \tag{31}$$

and the dynamic shift is

$$\delta_a = \wp \sum_{\mathbf{k}} \frac{|\langle g,g;1_{\mathbf{k}}|H_I'|a;\{0_{\mathbf{k}}\}\rangle|^2}{\omega_{eg}' + \Delta E_a^{\mathrm{sta}} - \omega_k}. \tag{32}$$

In these formulas, $\Gamma_{eg} = \frac{d_{eg}^2 \omega_{eg}^3}{3\pi\varepsilon_0 c^3}$ is the single-atom decay rate from $|e\rangle$ to $|g\rangle$, and $\wp$ stands for principle value. In Eq. (29), we have used

$$\int_{-\infty}^{t} dt' e^{ix(t-t')} = \pi\delta(x) + i\wp\frac{1}{x}. \tag{33}$$

Equation (30) is calculated in detail in the Appendix. Note that the decay rate of the antisymmetric state is modified by the function of $D(x_{12},\eta)$ with $x_{12} = \omega_{eg} r_{12}/c$ and $\eta$ the angle between the dipole moment and the vector $\mathbf{r}_2 - \mathbf{r}_1$, as shown in Fig. 1. From Eq. (29), the probability amplitude of state $|a;\{0_{\mathbf{k}}\}\rangle$ is

$$C_a(t) = C_a(0) e^{-(\frac{\Gamma_a}{2} + i\delta_a)t}. \tag{34}$$

Similarly, we can get the probability amplitude of $|s;\{0_{\mathbf{k}}\}\rangle$,

$$C_s(t) = C_s(0) e^{-(\frac{\Gamma_s}{2} + i\delta_s)t}, \tag{35}$$

in which the decay rate and the dynamic shift for the symmetric state are

$$\Gamma_s = 2\pi \sum_{\mathbf{k}} |\langle g,g;1_{\mathbf{k}}|H_I'|s;\{0_{\mathbf{k}}\}\rangle|^2 \delta\left(\omega_{eg}' + \Delta E_s^{\mathrm{sta}} - \omega_k\right)$$
$$= \Gamma_{eg}[1 + D(x_{12},\eta)], \tag{36}$$

$$\delta_s = \wp \sum_{\mathbf{k}} \frac{|\langle g,g;1_{\mathbf{k}}|H_I'|s;\{0_{\mathbf{k}}\}\rangle|^2}{\omega_{eg}' + \Delta E_s^{\mathrm{sta}} - \omega_k}. \tag{37}$$

Equations (34) and (35) show that the symmetric and antisymmetric states decay exponentially with their own decay rates $\Gamma_{a,s}$ and dynamic shifts $\delta_{a,s}$.

### A. The decay rates

The modification of the decay rates is completely determined by $D(x,\eta)$, which is a dimensionless function of the renormalized interatomic distance $x_{12} = \omega_{eg} r_{12}/c$ and the angle $\eta$. In Fig. 2, we plot the functions $D(x_{12},\eta)$ for $\eta = 0$ and $\pi/2$. It reaches its maximum value of 1 as $x \to 0$ (i.e., when the atomic distance tends to zero); the decay rate of the symmetric state will be double the decay rate of a single atom, while the decay rate of the antisymmetric state tends to zero. Note that $D(x,\eta)$ may become negative as the distance increases [see $D(x,\pi/2)$ in Fig. 2], which tells us that the antisymmetric state may decay faster than the symmetric state [see Eqs. (30) and (36)]. Therefore, the symmetric state is not necessarily superradiant and the antisymmetric state is not necessarily subradiant. The classical correspondence for this phenomenon is quite clear: The atoms are regarded as dipole antennas. When the distance between the atoms is much shorter than the wavelength, and if they radiate in phase (symmetric state), the radiation fields interference constructively, and thus energy is emitted faster. However, if the distance is comparable with or even larger than the wavelength, the out-of-phase configuration (antisymmetric state), rather than the in-phase configuration, may lead to constructive interference and thus decays faster. Because the interference patterns, as well as the emitting efficiency, are also dependent of the angle $\eta$, it is natural that the decay rate is also dependent of this angle, as shown in Fig. 3(a).

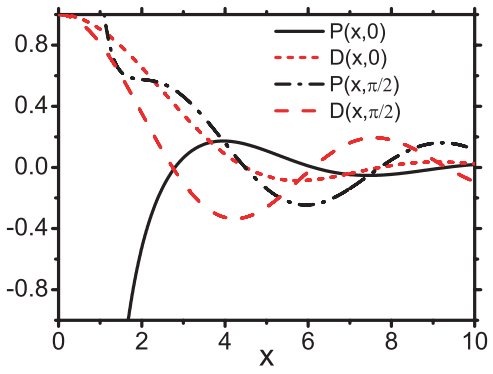


FIG. 2. (Color online) $D(x,\eta)$ and $P(x,\eta)$ for $\eta = 0$ and $\pi/2$.

### B. The Lamb shift

By combining Eqs. (17), (16), (18), and (32), the total energy shift of the antisymmetric state is

$$\Pi_a = E_a^{\mathrm{nd}} + \Delta E_a^{\mathrm{sta}} + \delta_a = E_a^{\mathrm{nd}} - (E_{d-d} + E_{ia}) + \delta_a, \tag{38}$$

which is composed of three contributions, the nondynamic shift $E_a^{\mathrm{nd}} = E_e^{\mathrm{nd}} + E_g^{\mathrm{nd}}$, the static nondynamic shift $\Delta E_a^{\mathrm{sta}}$ (including the electrostatic and quasi-static shifts), and the dynamic shift $\delta_a$. The result of this summation is (see the Appendix)

$$\Pi_a = E_a^{\mathrm{nd}} + \Delta E_a^{\mathrm{sta}} + \delta_a$$
$$= \left(E_e^{\mathrm{nd}} + \Delta_{eg}\right) + E_g^{\mathrm{nd}} - \frac{\Gamma_{eg}}{2} P(x_{12},\eta)$$
$$= \Delta_e^{\mathrm{Lamb}} + \Delta_g^{\mathrm{Lamb}} - \frac{\Gamma_{eg}}{2} P(x_{12},\eta), \tag{39}$$

where $\Delta_e^{\mathrm{Lamb}} (= E_e^{\mathrm{nd}} + \Delta_{eg})$ and $\Delta_g^{\mathrm{Lamb}}$ are the Lamb shifts of the excited and ground state of a single atom, respectively, $\Delta_{eg}$ is the dynamic shift of the excited state of a single atom, and $P(x_{12},\eta)$ is the dimensionless function

$$P(x,\eta) = \frac{3}{2x}\left[-\cos x \sin^2\eta + \left(\frac{\sin x}{x} + \frac{\cos x}{x^2}\right)(1 - 3\cos^2\eta)\right]. \tag{40}$$

The physics of Eq. (39) is clear. The first two terms are due to the components ($|e\rangle$ and $|g\rangle$) of the state $|a\rangle$ and the last term is dependent of $\mathbf{r}_{12}$ due to the direct dipole interaction and the virtual and real photon exchange between the two atoms. By

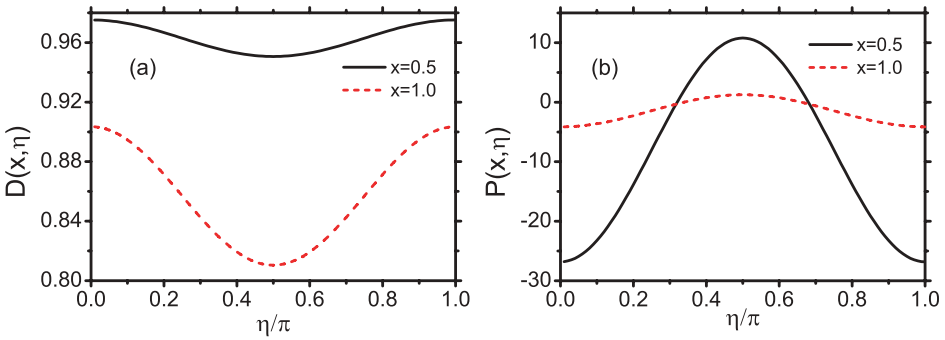


FIG. 3. (Color online) (a) $D(x,\eta)$ and (b) $P(x,\eta)$ for $x = 0.5$ and 1.0.

combining Eqs. (13), (16), (18), and (37), the total energy shift of the symmetric state is

$$\Pi_s = E_s^{\rm nd} + \Delta E_s^{\rm sta} + \delta_s = E_s^{\rm nd} + (E_{d-d} + E_{ia}) + \delta_s = \Delta_e^{\rm Lamb} + \Delta_g^{\rm Lamb} + \frac{\Gamma_{eg}}{2} P(x_{12},\eta). \quad (41)$$

The energy difference between these two states is

$$\Pi_s - \Pi_a = \Gamma_{eg} P(x_{12},\eta), \quad (42)$$

which tells us that the splitting between the symmetric and antisymmetric states is determined by $P(x_{12},\eta)$.

In Fig. 2, we plot $P(x,\eta)$ as a function of distance for $\eta = 0$ and $\pi/2$. It is shown that $P(x,\eta)$ is divergent with $1/x$. This is because the interaction energy is divergent as the distance between atoms gets to zero. In the limit $x \to 0$, $P(x,\eta)$ tends to $+\infty$ for $\eta = 0$ while it tends to $-\infty$ for $\eta = \pi/2$. This means that the dipole radiation fields do not have spherical symmetry and the interaction strength and energy are $\eta$-dependent. From the classical point of view, this comes from the fact that the interaction energies of the dipoles have different signs for different configurations, which will be more clearly discussed for the spectrum in Fig. 6. We also present this angle dependence in Fig. 3(b) for two distances $x = 0.5$ and 1.0.

### C. The emission spectra

If we substitute Eqs. (34) and (35) into the integration of Eq. (27), the probability amplitude for photon state $|1_{\mathbf{k}}\rangle$ in the long-time limit is

$$C_{\mathbf{k}}(\infty) = \frac{\sqrt{2}}{2} V_{eg,\mathbf{k}} e^{-i\mathbf{k}\cdot\mathbf{r}_1} \times \left[ \frac{C_a(0)(1 - e^{i\mathbf{k}\cdot\mathbf{r}_{12}})}{X_A} + \frac{C_s(0)(1 + e^{i\mathbf{k}\cdot\mathbf{r}_{12}})}{X_S} \right] \quad (43)$$

with

$$X_A = \delta_k + \frac{\Gamma_{eg}}{2} P(x_{12},\eta) + i\Gamma_a, \quad (44)$$

$$X_S = \delta_k - \frac{\Gamma_{eg}}{2} P(x_{12},\eta) + i\Gamma_s, \quad (45)$$

where the detuning is $\delta_k = \omega_k - \omega_{eg}^s$ and $\omega_{eg}^s = \omega_{eg}' + \Delta_{eg} = (\omega_e + \Delta_e^{\rm Lamb}) - (\omega_g + \Delta_g^{\rm Lamb})$ is the single atomic transition frequency including the Lamb shift [11]. Note that the positions of the two peaks in Eq. (44) and (45) are at $\omega_k = \omega_{eg}^s \mp \frac{\Gamma_{eg}}{2} P(x_{12},\eta)$, respectively, which is separated by $\Gamma_{eg} P(x_{12},\eta)$ due to the exchange of photons between the two atoms. This separation increases with the decrease of the distance $\mathbf{r}_{12}$.

The electric field at position $\mathbf{r}$ and time $t$ ($\hbar = 1$) is

$$\langle\{0_{\mathbf{k}}\}|\mathbf{E}^{(+)}(\mathbf{r},t) \sum_{\mathbf{k}} C_{\mathbf{k}}(\infty)|1_{\mathbf{k}}\rangle = \langle\{0_{\mathbf{k}}\}| \sqrt{\frac{1}{2\varepsilon_0 V}} \sum_{\mathbf{k}} \sqrt{\omega_k} a_{\mathbf{k}} \hat{\mathbf{e}}_{\mathbf{k}} e^{-i\omega_k t + i\mathbf{k}\cdot\mathbf{r}} \sum_{\mathbf{k}} C_{\mathbf{k}}(\infty)|1_{\mathbf{k}}\rangle \approx \frac{1}{2\pi} \int_0^\infty d\omega_k e^{-i\omega_k t} \mathbf{B}(\mathbf{r},\omega_k), \quad (46)$$

where

$$\mathbf{B}(\mathbf{r},\omega_k) = -\frac{\sqrt{2}\omega_{eg} \hat{\mathbf{r}}_1' \times (\mathbf{d}_{eg} \times \hat{\mathbf{r}}_1')}{4i\pi\varepsilon_0 c^2 r_1'} e^{ikr_1'} \left( \frac{2\omega_{eg}\omega_k}{\omega_k + \omega_{eg}} \right) \times \left[ \frac{C_a(0)(1 - e^{ix_{12}\cos\alpha})}{X_A} + \frac{C_s(0)(1 + e^{ix_{12}\cos\alpha})}{X_S} \right]. \quad (47)$$

In Eqs. (46) and (47), we have only retained the outward wave with the phase factor $e^{ikr_i' - i\omega_k t}$ in which $\mathbf{r}'_i = \mathbf{r} - \mathbf{r}_i \equiv \hat{\mathbf{r}}'_i r'_i$ denotes the displacement from the $i$th atoms to the observation point, and we have also neglected higher order terms of $O(1/\Delta r_i^2)$ because they decay to zero rapidly in the far field. We have made the approximation $r_1' \approx r_2'$ except in the exponential terms $e^{ik(r_2' - r_1')} \approx e^{ix_{12}\cos\alpha}$ with $x_{12} = \omega_{eg}|\mathbf{r}_2 - \mathbf{r}_1|/c$ and $\alpha$ being the angle between $\mathbf{r}_{12}$ and $\mathbf{r}_1'$. The relations between the detector and the two atoms are schematically plotted in Fig. 4.

The factor $\frac{2\omega_{eg}}{\omega_k + \omega_{eg}}$ comes from the fact that the atom will decay to the ground state of the atom-field system rather than the direct product of the bare-atom ground state and vacuum state. However, the spectrum is centralized near the single-atom

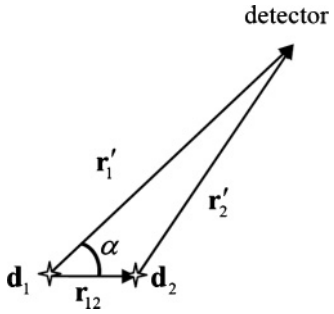


FIG. 4. The relation between the detector and two atoms.

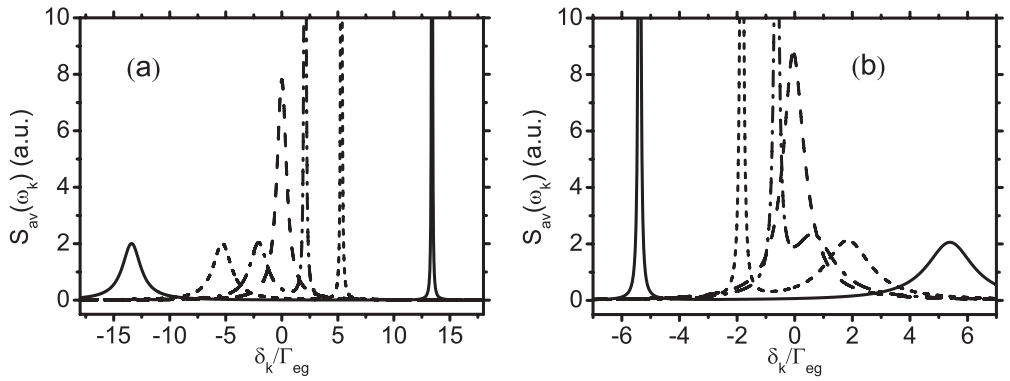


FIG. 5. The average spectrum (in arbitrary units) for (a) $\eta = 0$ and (b) $\eta = \pi/2$; $x_{12} = 0.5$ (solid), 0.7 (short dash), 1.0 (dash dot), and 5.0 (dash).

transition frequency where $\omega_k \approx \omega_{eg}$. Therefore, we can make a very good approximation, $\frac{2\omega_{eg}\omega_k}{\omega_k+\omega_{eg}} \approx \omega_{eg}$. The spectrum is

$$S(\omega_k,x_{12},\alpha) \propto |\mathbf{B}(\mathbf{r},\omega_k)|^2 \propto \left| \frac{C_a(0)(1-e^{ix_{12}\cos\alpha})}{X_A} + \frac{C_s(0)(1+e^{ix_{12}\cos\alpha})}{X_S} \right|^2, \tag{48}$$

which has two peaks at $\omega_k = \omega_{eg}^s \mp \frac{\Gamma_{eg}}{2} P(x_{12},\eta)$, and there are interferences between the spectra of $|a\rangle$ and $|s\rangle$. The spectra also depend on the observation point characterized by $\alpha$. We average over solid angles:

$$\begin{aligned} &S_{\rm av}(\omega_k,x_{12}) \\ &\propto \frac{1}{4\pi}\int_0^{2\pi} d\varphi \int_0^{\pi} \sin\alpha d\alpha \\ &\quad \times \left| \frac{C_a(0)(1-e^{ix_{12}\cos\alpha})}{A} + \frac{C_s(0)(1+e^{ix_{12}\cos\alpha})}{S} \right|^2 \\ &= \frac{2|C_a(0)|^2}{|A|^2}\left(1-\frac{\sin x_{12}}{x_{12}}\right) + \frac{2|C_s(0)|^2}{|S|^2}\left(1+\frac{\sin x_{12}}{x_{12}}\right). \end{aligned} \tag{49}$$

Note that although there is interference (constructive or destructive) between the spectra of the symmetric and antisymmetric states for any particular angle $\alpha$ [see the two terms in Eq. (48)], the average of this interference effect is zero, as shown in (49). If we initially prepare one of the atoms on the excited state and the other on the ground state, that is,

$$|\Psi(0)\rangle = |e,g;0_{\mathbf{k}}\rangle = \frac{1}{\sqrt{2}}|a;0_{\mathbf{k}}\rangle + \frac{1}{\sqrt{2}}|s;0_{\mathbf{k}}\rangle, \tag{50}$$

we have $C_a(0) = C_s(0) = \frac{1}{\sqrt{2}}$. In Fig. 5, we plot the average spectra for (a) $\eta = 0$ and (b) $0.5\pi$. When the atoms are placed very near each other, the interaction between the two atoms splits the spectrum into two peaks, one due to the symmetric state and the other due to the antisymmetric state. As the distance increases, the two peaks merge into one peak and finally, the spectrum tends to be the single-atom Lorentzian peak. Moreover, in Fig. 5(a), the symmetric state (wide peak) is red-shifted and the antisymmetric state (narrow peak) is blue-shifted, while in Fig. 5(b), the symmetric state is blue-shifted and the antisymmetric state is red-shifted. This means that the symmetric state has lower energy for $\eta = 0$ but higher energy for $\eta = 0.5\pi$. We can also see this $\eta$ dependence of the shifts from the $P(x,\eta)$ in Fig. 3(b), where $P(x,\eta = 0)$ is negative and $P(x,\eta = \pi/2)$ is positive. The classical correspondence of this angular dependence is easy to understand. We plot the configurations for in-phase and out-of-phase dipole antennas in Fig. 6. If $\eta = 0$, the two dipoles in the symmetric state [see Fig. 6(a)] oscillate in phase. In this configuration they obviously have attractive interaction. In contrast, the two dipoles in the antisymmetric state [see Fig. 6(b)] oscillate completely out of phase and have a repulsive interaction. This means that the symmetric state has lower energy (red shift) and the antisymmetric state has higher energy (blue shift), as shown in Fig. 5(a). If $\eta = \pi/2$, the symmetric state [see Fig. 6(c)] has a repulsive interaction with higher energy and the antisymmetric state [see Fig. 6(d)] has an attractive interaction with lower energy, and thus the symmetric state is blue-shifted and the antisymmetric state is red-shifted, as shown in Fig. 5(b). In Fig. 7, we plot the angular dependence of the spectrum for fixed atomic distance. It is clear that there is a level crossing for these two states as $\eta$ changes, which can also be seen from Fig. 3(b), where the sign of $P(0.5,\eta)$ changes with $\eta$.

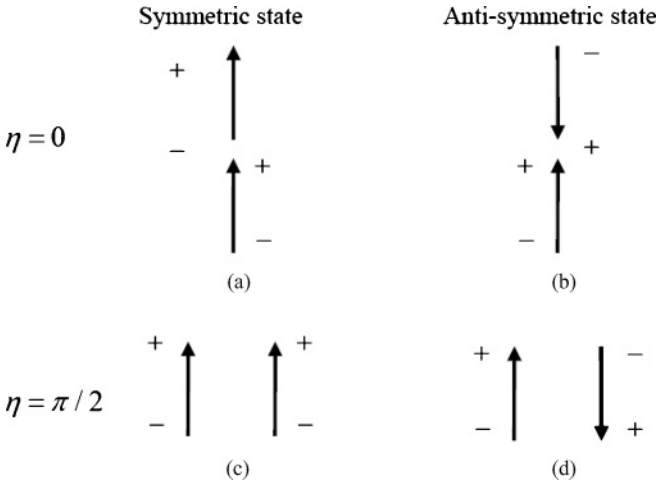


FIG. 6. The classical configurations for symmetric states [(a) and (c)] and antisymmetric states [(b) and (d)] with $\eta = 0$ [(a) and (b)] and $\pi/2$ [(c) and (d)].

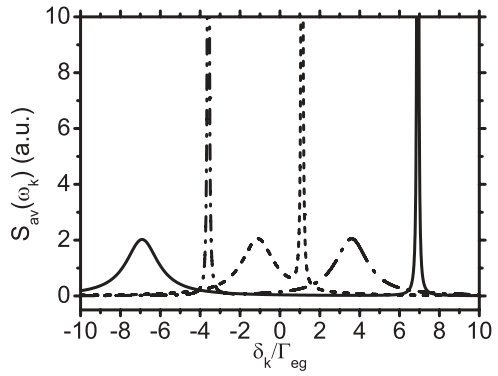


FIG. 7. The average spectra for $x_{12} = 0.5$ with $\eta = 0.2\pi$ (solid), $0.3\pi$ (short dash), and $0.4\pi$ (dash dot).

In some special observation directions, we may observe Fano spectra. Here we suppose both $C_a(0)$ and $C_s(0)$ are real; if the observation angle $\alpha_d$ satisfies

$$\tan\frac{x_{12}\cos\alpha_d}{2} = \frac{C_s(0)}{C_a(0)}\frac{-P(x_{12},\eta)\pm\sqrt{P^2(x_{12},\eta)+D^2(x_{12},\eta)-1}}{1+D(x_{12},\eta)}, \tag{51}$$

we may observe dark points at

$$\delta_k^0 = \mp\frac{\Gamma_{eg}}{2}\sqrt{P^2(x_{12},\eta)+D^2(x_{12},\eta)-1}. \tag{52}$$

In Fig. 8, we plot the spectrum with $\eta = \pi/2$, $\alpha = 1.73$, and $x_{12} = 1$, which satisfies Eq. (51); we can see a completely dark point due to the interference between the states $|e,g;0_{\mathbf{k}}\rangle$ and $|g,e;0_{\mathbf{k}}\rangle$ [13]. However, there are differences between our results and the results of Ref. [13], where a three-level atom with two parallel electric dipole transitions is investigated and the dark point in the spectrum can be observed from all directions. The three levels in our system belong to two atoms with a finite distance between them. The distance displays decoherence, making the quantum interference strength smaller than one. Moreover, spherical symmetry is broken, which is replaced by cylindrical symmetry, and the spectra are $\alpha$ dependent. Only in some particular observation directions ($\alpha_d$) can a complete dark point be observed for some particular frequency. This dark point comes not only from the quantum interference of the

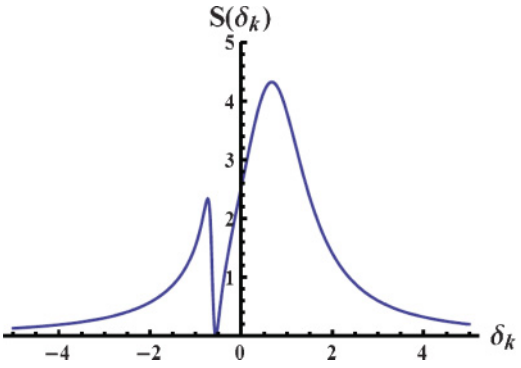


FIG. 8. (Color online) Fano spectrum (in arbitrary units) with a dark point with $\eta = \pi/2$, $x_{12} = 1$, and $\alpha = 1.73$.

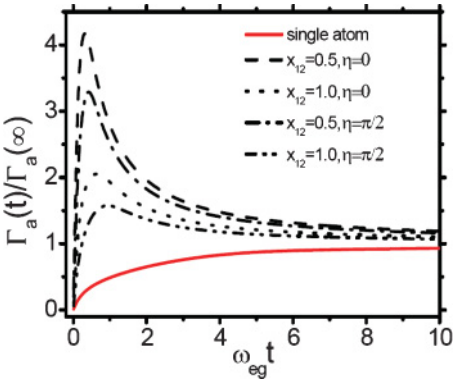


FIG. 9. (Color online) The time-dependent decay rates normalized with their respective long-time limits for the antisymmetric state. The red solid curve is for the case of a single atom, the decay rate of the excited state, $\Gamma_0(t)/\Gamma_0$.

two atomic transitions but also from the classical interference between two radiating dipoles.

## V. SHORT-TIME EVOLUTION

Now, we consider the time evolution of the decay rates, $\Gamma_{a,s}(t)$. In our previous studies for the case of a single atom, the decay rate shows the quantum Zeno (QZE) and quantum anti-Zeno effect (QAZE) in free vacuum [9] as well as in modified vacuum [11]. The modification of the density of states can greatly modulate the short-time behavior of the system. Here, we will extend the discussion to the two-atom system. Because the nondynamic shift and electrostatic shift are very small compared with the transition frequency, we neglect these shifts in the differential equations of Eq. (28):

$$\begin{aligned}\dot{C}_a(t) &= -\int_0^t dt'\sum_{\mathbf{k}}|\langle g,g;1_{\mathbf{k}}|H_I'|a;\{0_{\mathbf{k}}\}\rangle|^2 e^{i(\omega_{eg}-\omega_k)(t-t')}C_a(t')\\ &\approx -C_a(0)\frac{\Gamma_{eg}}{2\pi}\int_0^\infty d\omega_k G(\omega_k,x_{12},\eta)\int_0^t dt' e^{i(\omega_{eg}-\omega_k)(t-t')},\end{aligned} \tag{53}$$

where

$$G_a(\omega_k,x_{12},\eta) = \frac{4\omega_{eg}\omega_k}{(\omega_{eg}+\omega_k)^2}\left[1-D\left(\frac{\omega_k}{\omega_{eg}}x_{12},\eta\right)\right] \tag{54}$$

is the effective density of states for the antisymmetric state. In Eq. (53), we have approximated that the change of the probability amplitude is negligible for the very short time scale we are interested in, which is quite true for the weak coupling strength between atoms and the vacuum fields [14]. From Eq. (53), we can get the effective decay rate defined as

$$|C_a(t)|^2 = |C_a(0)|^2 e^{-\Gamma_a(t)t}. \tag{55}$$

The explicit expression of the effective decay rate is [9]

$$\Gamma_a(t) = \frac{\Gamma_{eg}}{2\pi}\int_0^\infty d\omega G_a(\omega,x_{12},\eta)\frac{4\sin^2[(\omega-\omega_{eg})t/2]}{(\omega-\omega_{eg})^2 t}. \tag{56}$$

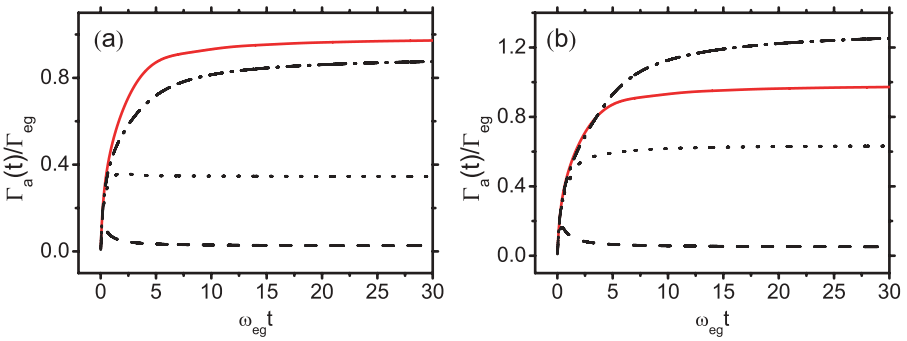


FIG. 10. (Color online) The time-dependent decay rate of the antisymmetric state. (a) $\eta = 0$ and (b) $\eta = \pi/2$, with $x_{12} = 0.5$ (dash), 2.0 (dot), and 4.0 (dash dot). The red solid curve is for the single-atom decay rate.

In Fig. 9, we plot the time-dependent decay rates normalized with their long-time limit in the free vacuum, $\Gamma_a(t)/\Gamma_a(\infty)$. It is clear that we have strong QAZE for the antisymmetric state, if the distances between two atoms are small compared with the transition wavelength. In contrast, a single atom only has QZE (red solid line). In Fig. 10, we plot the evolution of the decay rates for various distances with $\eta = 0$ and $\eta = \pi/2$. It seems that the QAZE disappears as the distance increases, because the quantum interference effect between the two atomic transitions decreases quickly as the distance increases. In a previous paper [11], we have demonstrated that the reduction of the DOS at the transition frequency may induce the QAZE. Here, the QAZE also comes from the reduction of the effective DOS of the antisymmetric state [Eq. (54)] with short interatomic distance, however, not by the modification of the vacuum, but by the interference between two atoms.

We can also get the time-dependent decay rate for the symmetric state:

$$\Gamma_s(t) = \frac{\Gamma_{eg}}{2\pi}\int_0^\infty d\omega G_s(\omega, x_{12}, \eta)\frac{4\sin^2[(\omega-\omega_{eg})t/2]}{(\omega-\omega_{eg})^2 t}, \tag{57}$$

where

$$G_s(\omega_k, x_{12}, \eta) = \frac{4\omega_{eg}\omega_k}{(\omega_{eg}+\omega_k)^2}\left[1 + D\left(\frac{\omega_k}{\omega_{eg}}x_{12}, \eta\right)\right]. \tag{58}$$

In Fig. 11, we plot $\Gamma_s(t)$ under various conditions. However, in contrast to the antisymmetric state, the QAZE appears to be very weak at $x_{12} = 4.0$ and $\eta = \pi/2$. This also comes from a small reduction of the effective DOS, because, at this distance, the function $D(4.0, \pi/2) < 0$ (see Fig. 2).

## VI. SUMMARY

In this paper, we have extended the unitary transformation method to a system of two multilevel atoms, where the self-energy is subtracted from the Hamiltonian at the beginning. The Lamb shift, which appears naturally in our calculations, can be classified into nondynamic shifts and dynamic shifts. Both of them include the contributions from a single atom and between the two atoms (the interatomic shifts, which do not exist in the one-atom case). In the long-time limit, the spectra are investigated. The peaks and their blue and red shifts have clear classical correspondence. We also investigate the short-time evolution of the system and the QZE and AQZE are found.

## ACKNOWLEDGMENTS

This work is supported by the RGC of the Hong Kong government (CUHK403609 and HKBU203107), the FRG of Hong Kong Baptist University, and CUHK 2060360 of the Chinese University of Hong Kong. H. Zheng is supported partly by the National Natural Science Foundation of China (Grant No. 10734020).

## APPENDIX: SHIFT AND DECAY RATE OF THE SYMMETRIC AND ANTISYMMETRIC STATES

To calculate the total shift of antisymmetric state in Eq. (44), we first evaluate the shift brought by the transverse field,

$$\begin{aligned} -E_{ia} + \delta_a &= \langle a|H_{ia}|a\rangle + \wp\sum_{\mathbf{k}}\frac{|\langle g,g;1_{\mathbf{k}}|H_I'|a;\{0_{\mathbf{k}}\}\rangle|^2}{\omega_{eg}' - E_{ia} - E_{d-d} - \omega_k} \\ &\approx \sum_{\mathbf{k}}\frac{2|g_{\mathbf{k};eg}|^2\xi_{k;eg}}{\omega_k}(2-\xi_{k;eg})e^{i\mathbf{k}\cdot(\mathbf{r}_1-\mathbf{r}_2)} \\ &\quad + \wp\sum_{\mathbf{k}}\frac{1}{\omega_{eg}-\omega_k}\frac{1}{2}|V_{eg,\mathbf{k}}|^2|(e^{-i\mathbf{k}\cdot\mathbf{r}_1} - e^{-i\mathbf{k}\cdot\mathbf{r}_2})|^2 \end{aligned}$$

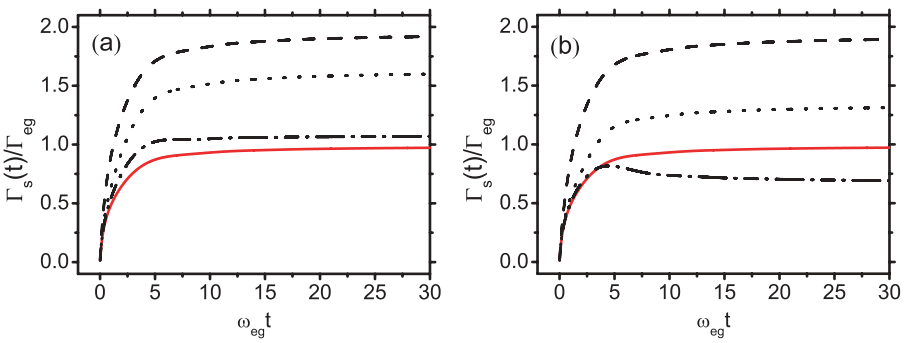


FIG. 11. (Color online) The time-dependent decay rate of the symmetric state. (a) $\eta = 0$ and (b) $\eta = \pi/2$ with $x_{12} = 0.5$ (dash), 2.0 (dot), and 4.0 (dash dot). The red solid curve is for the single-atom decay rate.

$$= \frac{d_{eg}^2\omega_{eg}^2}{6\pi^2\varepsilon_0 c^3}\int_0^\infty \frac{2(\omega_k+2\omega_{eg})\omega_k}{(\omega_k+\omega_{eg})^2}D(kr_{12},\eta)d\omega_k + \frac{d_{eg}^2\omega_{eg}^2}{6\pi^2\varepsilon_0 c^3}\wp\int_0^\infty \frac{\omega_k}{\omega_{eg}-\omega_k}\frac{4\omega_{eg}^2}{(\omega_k+\omega_{eg})^2} \times [1-D(kr_{12},\eta)]d\omega_k = \Delta_{eg} - \frac{d_{eg}^2\omega_{eg}^2}{6\pi^2\varepsilon_0 c^3}\wp\int_0^\infty \frac{2\omega_k^2}{\omega_{eg}^2-\omega_k^2}D(kr_{12},\eta)d\omega_k, \quad \text{(A1)}$$

where

$$\Delta_{eg} = \frac{d_{eg}^2\omega_{eg}^2}{6\pi^2\varepsilon_0 c^3}\wp\int_0^\infty \frac{\omega_k}{\omega_{eg}-\omega_k}\frac{4\omega_{eg}^2}{(\omega_k+\omega_{eg})^2}d\omega_k \quad \text{(A2)}$$

is the dynamic shift of a single atom. The summation of nondynamic shift $E_e^{\rm nd}$ and dynamic shift $\Delta_{eg}$ gives the total Lamb shift of the excited state $|e\rangle$ [11]. We have neglected the various shifts in the principle integration because they are all tiny compared with the transition frequency, and we have changed the summation over $\mathbf{k}$ into an integration [7],

$$\sum_{\mathbf{k}} g_{\mathbf{k};ij}^2 e^{i\mathbf{k}\cdot\mathbf{r}_{12}} \to \frac{d_{eg}^2\omega_{eg}^2}{6\pi^2\varepsilon_0 c^3}\int_0^\infty \omega_k D(kr_{12},\eta)d\omega_k, \quad \text{(A3)}$$

where $D(x,\eta)$ is defined in Eq. (31). The integration gives

$$\frac{d_{eg}^2\omega_{eg}^2}{6\pi^2\varepsilon_0 c^3}\wp\int_0^\infty \frac{2\omega_k^2}{\omega_{eg}^2-\omega_k^2}D(kr_{12},\eta)d\omega_k = \frac{\Gamma_{eg}}{2}\frac{3}{2x_{12}}\left[-\cos x_{12}\sin^2\eta + \left(\frac{\sin x_{12}}{x_{12}} - \frac{1-\cos x_{12}}{x_{12}^2}\right)\times(1-3\cos^2\eta)\right]$$

$$= \frac{\Gamma_{eg}}{2}P(x_{12},\eta) - \frac{d_{eg}^2\omega_{eg}^3}{6\pi\varepsilon_0 c^3}\frac{3}{2}\frac{1}{(\omega_{eg}r_{12}/c)^3}(1-3\cos^2\eta) = \frac{\Gamma_{eg}}{2}P(x_{12},\eta) - \frac{d_{eg}^2}{4\pi\varepsilon_0 r_{12}^3}(1-3\cos^2\eta) = \frac{\Gamma_{eg}}{2}P(x_{12},\eta) - E_{d-d}. \quad \text{(A4)}$$

where $P(x_{12},\eta)$ is given in Eq. (40) and $E_{d-d} = \frac{d_{eg}^2}{4\pi\varepsilon_0 r_{12}^3}(1-3\cos^2\eta)$ can be directly obtained from Eq. (16). It is clear that a part of the shift induced by the transverse fields cancels the static dipole-dipole interaction energy. Combining Eq. (A1) and (A4), we get the terms in Eq. (39):

$$\Delta E_a^{\rm sta} + \delta_a = -E_{ia} - E_{d-d} + \delta_a = (-E_{ia}+\delta_a) - E_{d-d} = \Delta_{eg} - \left[\frac{\Gamma_{eg}}{2}P(x_{12},\eta) - E_{d-d}\right] - E_{d-d} = \Delta_{eg} - \frac{\Gamma_{eg}}{2}P(x_{12},\eta). \quad \text{(A5)}$$

The corresponding quantity for the symmetric state in Eq. (41) can be derived in a similar way. The decay rate of the antisymmetric state in Eq. (30) is

$$\Gamma_a = 2\pi\sum_{\mathbf{k}}|\langle g,g;1_{\mathbf{k}}|H_I'|a;\{0_{\mathbf{k}}\}\rangle|^2\delta(\omega_{eg}'-E_{ia}-E_{d-d}-\omega_k) \approx 2\pi\sum_{\mathbf{k}}\frac{1}{2}|V_{eg,\mathbf{k}}|^2|(e^{-i\mathbf{k}\cdot\mathbf{r}_1}-e^{-i\mathbf{k}\cdot\mathbf{r}_2})|^2\delta(\omega_{eg}-\omega_k) = \frac{d_{eg}^2\omega_{eg}^2}{3\pi\varepsilon_0 c^3}\int_0^\infty \frac{4\omega_k\omega_{eg}^2}{(\omega_k+\omega_{eg})^2}[1-D(kr_{12},\eta)]\delta(\omega_{eg}-\omega_k)d\omega_k = \Gamma_{eg}[1-D(x_{12},\eta)]. \quad \text{(A6)}$$

Equation (36) can be obtained in the same way.


[1] R. H. Dicke, Phys. Rev. **93**, 99 (1954).

[2] A. A. Svidzinsky, J. T. Chang, and M. O. Scully, Phys. Rev. Lett. **100**, 160504 (2008).

[3] S. Das, G. S. Agarwal, and M. O. Scully, Phys. Rev. Lett. **101**, 153601 (2008).

[4] M. O. Scully, Phys. Rev. Lett. **102**, 143601 (2009).

[5] J. W. Czarnik and P. R. Fontana, J. Chem. Phys. **50**, 4071 (1969).

[6] R. H. Lehmberg, Phys. Rev. A **2**, 883 (1970); **2**, 889 (1970).

[7] G. S. Agarwal, *Quantum Optics*, Springer Tracts in Modern Physics, Vol. 70, edited by G. Höhler (Springer-Verlag, Berlin, 1974).

[8] D. F. V. James, Phys. Rev. A **47**, 1336 (1993); J. Guo, *ibid.* **50**, R2830 (1994); J. P. Clemens, L. Horvath, B. C. Sanders, and H. J. Carmichael, *ibid.* **68**, 023809 (2003); H. Freedhoff, *ibid.* **69**, 013814 (2004); C. Genes and P. R. Berman, *ibid.* **73**, 053809 (2006); E. Akkermans, A. Gero, and R. Kaiser, Phys. Rev. Lett. **101**, 103602 (2008); P. G. Brooke, K-P. Marzlin, J. D. Cresser, and B. C. Sanders, Phys. Rev. A **77**, 033844 (2008).

[9] H. Zheng, S. Y. Zhu, and M. S. Zubairy, Phys. Rev. Lett. **101**, 200404 (2008); Z. H. Li, D. W. Wang, H. Zheng, S. Y. Zhu, and M. S. Zubairy, Phys. Rev. A **80**, 023801 (2009).

[10] A. B. Klimov and L. L. Sanchez-Soto, Phys. Rev. A **61**, 063802 (2000); A. B. Klimov, I. Sainz, and S. M. Chumakov, *ibid.* **68**, 063811 (2003).

[11] D. W. Wang, L. G. Wang, Z. H. Li, and S. Y. Zhu, Phys. Rev. A **80**, 042101 (2009).

[12] H. A. Bethe, Phys. Rev. **72**, 339 (1947).

[13] S. Y. Zhu, R. C. F. Chan, and C. P. Lee, Phys. Rev. A **52**, 710 (1995).

[14] A. G. Kofman and G. Kurizki, Nature (London) **405**, 546 (2000).